Damping of VFTO by RF Resonator and Nanocrystalline Materials

S. Burow, W. Köhler, S. Tenbohlen
University of Stuttgart
Stuttgart, Germany
simon.burow@ieh.uni-stuttgart.de

U. Straumann
ABB Switzerland Ltd
Zürich, Switzerland
ulrich.straumann@ch.abb.com

***Abstract*—Very fast transient overvoltages (VFTO) are a well known phenomena in gas insulated switchgears (GIS). The main reasons for VFTO are switching operations of disconnectors. Thereby several pre- or restrikes between the switching contacts occur and initiate steep voltage rises propagating inside the GIS. As VFTO cause several problems especially in ultra high voltage (UHV) GIS a reliable method for damping these transient voltages is in demand. Two new approaches are presented in this paper. A matched radio frequency resonator formed by shielding inside the GIS was investigated inside a high voltage experimental test setup. Also thin tapes of a nanocrystalline alloy wounded up to rings was tested. Addicted to the properties of the damping methods, the test setup and the damping method itself the first VFTO-amplitude was damped up to 20 percent. Even a higher damping is possible. Besides high voltage tests and their results this paper illustrates the theoretical background of both damping methods.**

Keywords—gas insulated switchgear (GIS); nanocrystalline material; radio frequency resonator; suppressing very fast transient overvoltage (VFTO)

I. Introduction

Gas insulated switchgears (GIS) are one of the most reliable components of electrical transmission networks and are suitable not only for special applications. By using sulfur hexafluoride (SF_6) as insulation medium the needed space for GIS is much less than for an air insulated switchgear (AIS). Further advantages of a GIS are an excellent reliability and less maintenance effort. As every part energized with high voltage is shielded by the enclosure, disturbances caused by external influences are almost impossible.

In a SF_6 atmosphere pre- or restrikes during switching operations and flashovers cause very steep voltage rises which initiate very fast transient overvoltages (VFTO). These electromagnetic waves propagate along the GIS and are reflected several times at discontinuities of the line impedance. The discontinuities are caused by changes in the coaxial arrangement of the GIS. The VFTO have a damped impulsive shape with spectral frequency contents from 100 kHz to 100 MHz. After approximately 1 µs, VFTO are mostly decayed. The amplitude of VFTO can reach up to three times the phase-to-ground voltage and the rise time is in a range of few nanoseconds near to the disconnector. In practice, the main sources for such VFTO are disconnector switching operations, where lots of pre- or restrikes occur during one switching process. Therefore steep voltage rises happen several times within a very short time and VFTO occur [1], [2], [3].

VFTO may cause high stress for the insulation system of GIS and other directly connected high voltage equipment. The risk of an insulation fault due to VFTO is increased for very high system voltage levels above 420 kV. In ultra high voltage (UHV) GIS the maximum VFTO can be higher than the rated lightning impulse withstand voltage (LIWV). Thus VFTO could be a limiting constraint for the dielectric design of UHV GIS [4]. Studies with different concepts for damping VFTO were carried out to reduce the dielectric stress for the SF_6-insulation system and high voltage equipment. Newest results of two promising options are presented in this paper.

The first new approach is a radio frequency (RF) resonator, which is located around the inner conductor of a GIS. Stimulated by the VFTO, the resonator gets into resonance and a special termination of the resonator should dissipate the VFTO energy. In a 550 kV GIS a test resonator was investigated. Especially different terminations and the influence of the dominant harmonic component of the VFTO were analyzed. The second promising concept bases upon rings of a nanocrystalline alloy placed around the GIS conductor. Rings of different material types and the influence of different number and size were investigated.

In the majority of cases the tests of both options were performed in a high voltage test setup with VFTO up to several hundreds of kilovolt. So the voltage stress was very similar to real VFTO in GIS. Influences on the damping effect and characteristics of the damping concepts will be illustrated in this paper.

II. Experimental Setup

The high voltage test setup mainly consists of a 550 kV GIS. A schematic diagram is shown in Fig. 1. The VFTO in the GIS are generated by a breakdown between the spark gap. For this purpose a standard high voltage impulse generator injects a surge voltage of several 100 kV via a bushing inside the GIS. The spark gap consists of two spherical electrodes and is situated in SF_6 atmosphere. As the surge voltage reaches the breakdown voltage of the spark gap, a sparkover occurs between the contacts and initiates the VFTO.

The authors would like to thank Dr M. Ferch and Mr. H. - J. Poess for the theoretical and material support during the investigation. Dr M. Ferch and Mr. H. - J. Poess are with MAGNETEC GmbH.

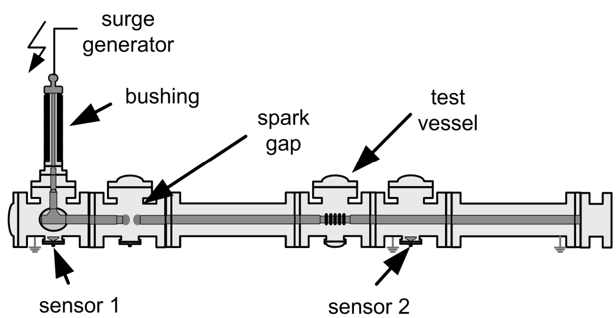

Fig. 1. Schematic diagram of the high voltage test setup: GIS with spark gap, capacitive voltage sensors and a flexible test vessel for different test installations.

Only the GIS compartments with the spark gap and the bushing are filled with SF_6. As it is easier to handle during the tests all other GIS parts are filled with air. By means of the SF_6 pressure and the distance of the spark gap, it is possible to control the breakdown voltage of the spark gap and thereby the amplitude of the resulting VFTO as well. Two possibilities to terminate the GIS at the bus duct end have been investigated. One was open termination, with ungrounded end of the inner conductor, whereby the transient voltage waves are reflected by a positive factor close to +1. The other termination used in the experiments was the connection of the inner conductor with two copper strips to the enclosure. Thus, the transient voltage waves are reflected by a negative factor close to -1. In a test vessel with one additional flange and a flexible inner conductor different testing objects (e.g. resonator and nanocrystalline rings) could easily be installed. On both sides of the test vessel capacitive voltage sensors are installed in a flange of the GIS enclosure, enabling very accurate measurement. The testing arrangement is presented in Fig. 2.

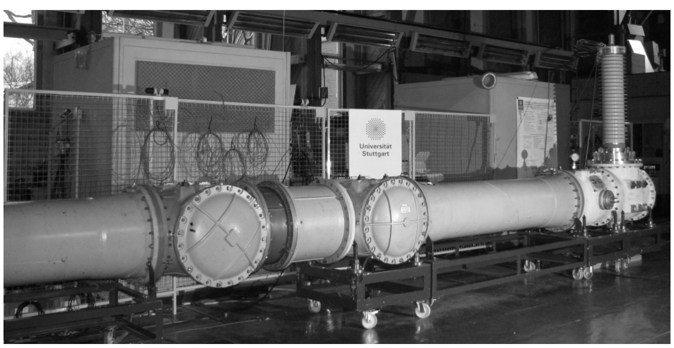

Fig. 2. The high voltage test setup in the laboratory of University of Stuttgart: ABB 550 kV GIS type ELK-3 with bushing.

By means of this setup VFTO with an amplitude up to 800 kV and more can be generated. The dominant harmonic component of the VFTO frequency spectrum is approximately 15 MHz for the GIS setup without ground strips (λ/2) and about 7.5 MHz for the GIS setup with a short-circuited (λ/4) termination. It is related to the reflection at the ends and the total length of the GIS.

For a precise measurement of VFTO a special developed capacitive voltage sensor was used. Two of these sensors were mounted inside the GIS. The sensors (see Fig. 3) consist mainly of a double layer board. The layer facing to the grounded GIS enclosure is connected to the enclosure by the flange and a copper EMC gasket directly. The top layer forms a capacitance to both the grounded layer and the inner conductor of the GIS (stray capacitance). This high frequency capacitive voltage divider has a divider ratio of some 10 000. The top layer is connected to a BNC-connector [4].

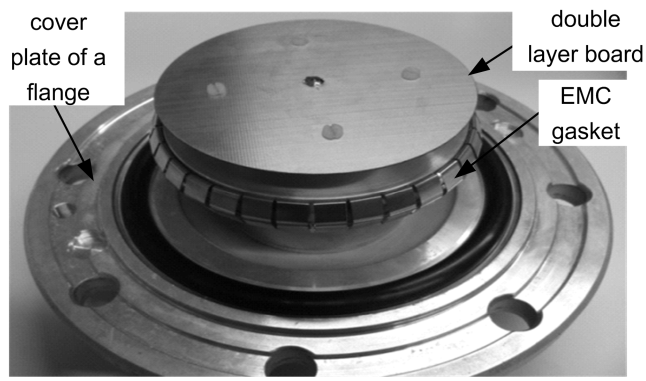

Fig. 3. The capacitive voltage sensor consisting of a double layer board, EMC gasket and cover plate of a flange.

The signals of the sensors are recorded by an oscilloscope (LeCroy waveRunner 104 MXi, used Bandwidth: 200 MHz). Before analysing the results, always 10 measurements were superimposed to avoid impacts caused by small variation of the breakdown voltage.

III. Radio Frequency Resonator for VFTO Damping

The first presented approach is based on the idea to use existing shielding parts inside the GIS for VFTO mitigation. If a shielding would be adjusted to a compact electromagnetic radio frequency (RF) resonator it could get stimulated by the VFTO. The challenge of this idea is not only the design of a suitable resonator. Also the dissipating of the VFTO energy must be investigated.

A. Theoretical consideration

Several shieldings of different sizes and at different locations are used inside a GIS to smooth the electric field. An example is the shielding around the energized parts of a disconnector switch. For a transformation of these cavities into a resonator, a gap in the screen around the GIS conductor is necessary (Fig. 4). Considering the gap in the shielding as a capacity C and the cavity of the resonator as an inductance L the resonator can be seen as a LC-resonant circuit with a resonant frequency f_R of [5]:

$$f_R = \frac{1}{2\pi\sqrt{LC}} \tag{1}$$

The capacity can be modified by the geometry of the gap. For example, it is possible to overlap the metal sheet of the shielding or adjust the distance of the gap. In the same way the inductance can be changed by a variation of the cavity. In that way it is possible to adapt the resonant frequency of the resonator to the dominant harmonic component of the VFTO. Of course the geometry of the resonator must not have an impact on the dielectric behaviour of the GIS.

If the resonant frequency of the resonator fits to the dominant harmonic component of the VFTO the resonator gets stimulated by the VFTO and energy is captured in the resonator. By a resistance in the resonant circuit energy could be adsorbed and thereby the VFTO damped. For an optimum mitigation the value of this resistor needs to have an ideal value. If it is too high and therefore the resonance circuit exceed the aperiodic oscillation, it constrains the resonance. A to small resistance adsorbs only less energy. The resistor can be located across the gap, which means in parallel to the capacity [6]. To prove this theoretical consideration a resonator model was built and several tests were carried out.

B. Measurements and results

The preliminary model of the resonator consists of two pipes which are arranged on the inner conductor of the GIS. Fig. 4 shows the test setup. By means of the shorter pipe an elongated gap between pipe and conductor is formed. This gap serves as a large capacity and ends up together with the inductance of the cavity in a resonance frequency equal to the dominant harmonic component of the VFTO (15 MHz). The resonance frequency of this arrangement was checked by a network analyzer.

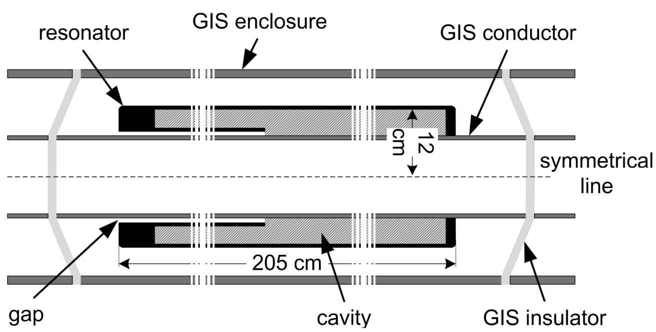

Fig. 4. Schematic diagram of the resonator in a GIS. Cavity and gap are matched to a resonance frequency of 15 MHz.

For the tests a resistor distributed around the gap is needed. Also an easy way to change its value is beneficial. Therefore a cavity was located in front of the gap as shown in Fig. 5. It was filled up with water of a certain salt content. The resistance could easily be adjusted by the salt content. The resistance value of this arrangement with each salt solution was measured by a RCL meter (PHILIPS PM 6303). By means of some fibre optic sensors around the gap flashovers inside the gap could be detected.

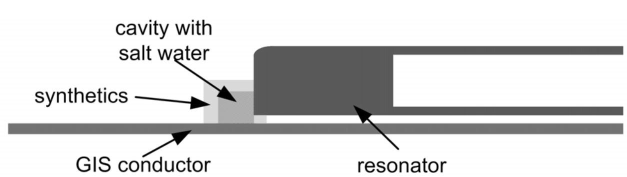

Fig. 5. Schematic diagram of the resistor between resonator and GIS conductor formed by a cavity filled up with salt water.

VFTO were generated and the influence of different resistor values on the resonator gap was investigated. Fig. 6 shows the voltage measured on sensor 2. For the reference VFTO the gap of the resonator was bridged by several metal pieces inside the gap. So the stimulation of the resonator was prevented. As an example measurements of a resistor with 12 Ω and 22 Ω are compared to the reference VFTO. A small damping could be achieved by the 12 Ω resistor. Nearly no damping effect is visible with the 22 Ω resistor. The analysis of the fibre optic sensors shows that only during the tests with the 22 Ω a flashover appears across the gap.

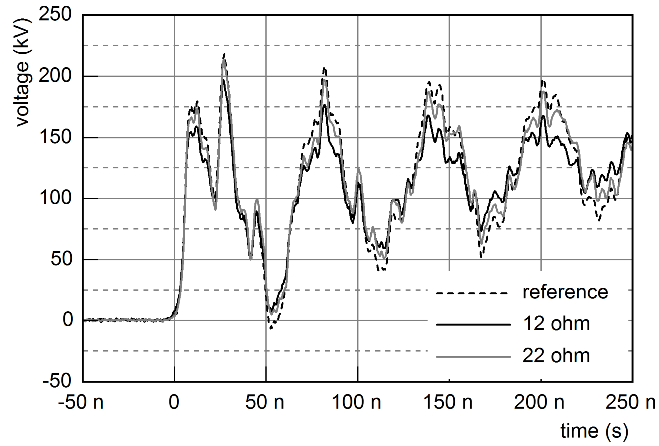

Fig. 6. VFTO measured on sensor 2; slight damping during the measurements with a resonator termination of 12 Ω (black line) and 22 Ω (grey line) in comparison to reference measurement with bridged resonator (dashed line).

Summing up all test results with different resistance values two facts are obvious. First, the damping effect increases with higher resistances. And second, if the resistance reaches a certain value a flashover in the gap occurs. Therefore the damping effect decreases very much. The breakdown voltage of the gap could be increased by SF_6 insulation. Thus higher resistors can be used and a better damping might be achieved. Also a wider gap would lead to a higher breakdown voltage. However, the capacitance formed by the gap would decrease in that case.

Also the impact of a deviating resonator resonance frequency from the dominant harmonic component of the VFTO was investigated during different tests. Therefore the

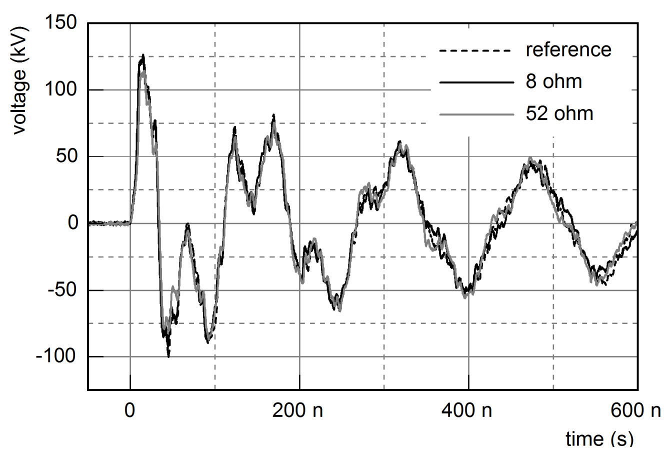

Fig. 7. VFTO measured on sensor 2 with dominate harmonic frequency of 7.5 MHz; no damping is visible between reference measurement with bridged resonator (dashed line) and measurements with a resonator termination of 8 Ω (black line) and 52 Ω (grey line).

inner conductor was grounded at the end of the GIS. This results in VFTO with a dominant harmonic component of about 7.5 MHz. The resonance frequency of the resonator is still 15 MHz. Fig. 7 compares VFTO with a dominant harmonic component of 7.5 MHz measured on sensor 2 with different resistors (8 Ω and 52 Ω) on the resonator gap and a bridged gap. No damping effect has been observed for this case.

These tests confirm that the resonant frequency of the resonator must be close to the dominant harmonic component of the VFTO. Their frequency spectrum varies and depends on the GIS dimension as well as on the switching conditions of the substation. To cover all dominant harmonics a resonator with a low quality factor or several resonators are necessary.

IV. Nanocrystalline Rings for VFTO Damping

A very good mitigation of VFTO was achieved by the second presented approach. Rings of a nanocrystalline alloy were arranged on the inner conductor of the GIS. Experiments with different ring types, different sizes and different numbers of rings were carried out.

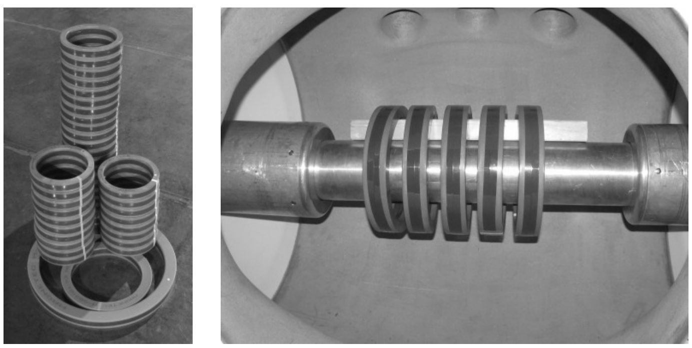

Fig. 8. Nanocrystalline rings with different sizes and characteristics (left) and 5 mounted rings inside the test vessel (right).

A. Material characteristics

The used alloy is based on iron (Fe) with silicium (Si), boron (B) and other additives [7]. By means of a rapid solidification technology the liquid metal is converted to very thin ribbons with a thickness of approximately 20 µm. The thin tape is winded up to rings. Finally a heat treatment with temperatures between 500 °C and 600 °C transforms the initially amorphous microstructure of the tape into the desired nanocrystalline state with fine crystalline grains embedded in an amorphous residual phase. The average grain diameter is between 10 nm and 40 nm. This material has very specific properties which could be adjusted by means of an external magnetic field during the heat treatment. Thereby the magnetic domains get aligned and the anisotropy of the material can be tuned. The analyzed rings have a transverse anisotropy to the direction of winding.

The magnetic saturation of nanocrystalline material is achieved by a magnetic field of only some A/m. However, the current inside a GIS causes magnetic fields several orders of magnitude higher than the saturation field strength. Therefore the rings are magnetic saturated and no energy loss is expected in the low frequency range (operating frequency). As different loss mechanisms exist in the frequency range of several MHz, mitigation of VFTO can be achieved. Three loss mechanisms could potentially be responsible for damping effects by nanocrystalline tape wound cores. They will be introduced shortly below:

Hysteresis losses are caused by the changing alignment of the magnetic domains by an external alternating magnetic field. The rotating process of the magnetic domains converts the rotating energy into thermal energy. The amount of energy is related to the area of the static hysteresis loop. As the static hysteresis loop of the used material is very slender this damping mechanism is almost insignificant. Furthermore magnetic saturation reduces the influence of this effect.

The VFTO create a very fast alternating magnetic field around the inner conductor in direction of the tape winding. By means of the steep field variation eddy currents are induced in the nanocrystalline tape. These currents cause power loss on the one hand and on the other hand a magnetic field orientated in opposite to the initial external field. This mechanism increases towards higher frequencies.

Micro eddy currents are the third damping mechanism. They are caused by the magnetization process of the magnetic domains. The used nanocrystalline material has a transverse anisotropy. Therefore the magnetization vectors of the domains are orientated at right angles to the direction of winding in a demagnetized state. A rising external field aligns the magnetization vector to the direction of the external field. By means of this rotation the field vector component, which is orientated transverse to the direction of the external field, gets varied. Thereby the micro eddy currents are induced.

Especially both eddy current phenomena are responsible for the damping effect. The high frequency components of the VFTO are required [8].

B. Measurements and results

Different rings with an external diameter between 20 cm and 50 cm and a rated relative permeability at 10 kHz between 8 000 and 45 000 were used (Fig. 8 left). The rings were installed centred on the GIS conductor as shown on the right side of Fig. 8. For all tests, the same setup was used as illustrated in Fig. 1 and Fig. 2. Also surge voltage, SF_6 pressure and gap distance were kept constant to ensure equal conditions.

The VFTO shown in Fig. 9 exemplify the mitigation of rings with a permeability of 45 000 and a diameter of 20 cm. Measurements with eight and three rings were compared to a reference voltage without rings. It is obvious that eight rings achieve a better damping effect than three rings. Focusing on the first VFTO peak the amplitude of the test with eight rings is reduced by about 20%. The damping effect on the second and all following peaks is even larger. These peaks are damped nearly completely. Further tests confirm that the damping effect increases approximately linear with the number of rings arranged around the GIS conductor. So it is possible to achieve a nearly complete mitigation of the first peak by using a sufficient number of rings.

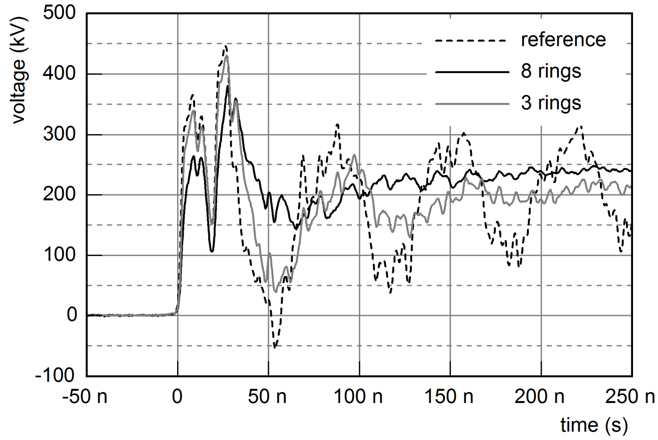

Fig. 9. VFTO measured on sensor 2; high damping was achieved by 8 rings (black line) in comparison to the reference without rings (dashed line). 3 rings leads to less damping (grey line).

The investigation with different ring diameters shows that it is possible to damp VFTO by means of all rings. But rings with a bigger diameter need much more volume of nanocrystalline material to reach a certain damping effect, as the magnetic flux is reduced with increasing radius.

Also rings with higher permeability lead to a better damping. Fig. 10 shows the damping effect of eight rings with a permeability of 45000 and eight rings with a permeability of 8000. As reference a VFTO without damping is also depicted.

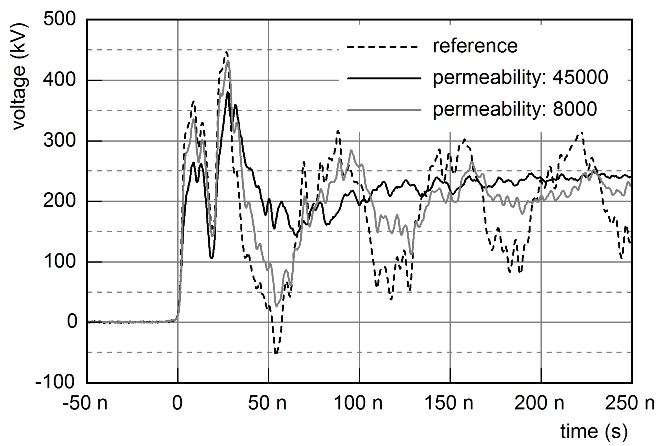

Fig. 10. VFTO measured on sensor 2; maximum damping effect was achieved by 8 rings with a permeability of 45 000 (black line) in comparison to 8 rings with a permeability of 8 000 (grey line) and the reference measurement without rings (dashed line).

Summing up these tests, a very good mitigation effect could be achieved by the nanocrystalline rings. Especially a test with all rings available during the first tests demonstrates the substantial mitigation capability. To reach certain VFTO mitigation the required number of rings is addicted to the permeability and the diameter of the rings. Detailed analysis show that the same damping effect could be reached with rings arranged under a shielding electrode. Therefore partial discharge (PD) inside the GIS could be avoided. It was also proved that the energy loss for the nominal frequency of the electric power supply is negligible.

V. Conclusion

The VFTO damping effect of two different new approaches was investigated in a high voltage test setup. Therefore VFTO with amplitudes from up to 800 kV were generated.

Measurement of RF resonators formed by shielding inside the GIS resulted in only weak damping in the investigated setup. The resonance frequency of the resonator can be adjusted to the main frequency component of the VFTO by changing the volume of the cavity or a gap in the shielding. A damping effect was achieved only, if the resonance frequency of the resonator fits very well to the main frequency component of the VFTO. Also a suitable value of the resistor across the gap was necessary. If it was too high, breakdowns occured on the gap. Therefore the gap gets bridged and the damping effect gets lost. Also small resistors lead to an only insufficient damping. Even so the actual results are not that promising, future investigation can reveal the capability of this damping solution and lead to a complete understanding of its work-principle.

A good damping effect was achieved by means of nanocrystalline rings. The first amplitude of the VFTO was damped up to 20 percent and all further peaks were mitigated nearly completely. These tape wound cores were located on the inner conductor of the GIS. Different parameters of the rings were investigated during different high voltage tests. High permeability of the rings and low diameter leads to an improved damping. The damping effect increases approximately linear with the number of rings arranged around the GIS conductor. No relevant energy loss was produced by the rings during rated voltage or current.

References

[1] J. Meppelink, K. Diederich, K. Feser, W. Pfaff, “Very Fast Transients in GIS”, IEEE Transactions on Power Delivery, Vol. 4, No. 1, pp. 223-223, Jan. 1989.

[2] CIGRÉ Brochure 456 Working Group A3.22, “Background of Technical Specifications for Substation Equipment Exceeding 800 kV AC”, April 2011.

[3] CIGRÉ Brochure 362 Working Group A3.22, “Technical Requirements for Substations Equipment Exceeding 800 kV - Field experience and technical specifications of Substation equipment up to 1200 kV”, December 2008.

[4] S. Burow, W. Köhler, S. Tenbohlen and U. Straumann, “Measurement System for Very Fast Transients in Gas Insulated Switchgear”, presented at the 31st Electrical Insulation Conf., Ottawa, Canada, June 2-5, 2013.

[5] J. Smajic, W. Holaus, A. Troeger, S. Burow, R. Brandl and S. Tenbohlen, “HF Resonators for Damping of VFTs in GIS”, International Conference on Power Systems Transients, Delft, Netherlands, 2011.

[6] S. Burow, U. Riechert, W. Köhler and S. Tenbohlen, “New mitigation methods for transient overvoltages in gas insulated substations”, in Proc. Stuttgarter Hochspannungssymposium, Stuttgart, Germany, 2012, pp. 169-181.

[7] MAGNETEC GmbH: http://www.magnetec.de/, product information “Cool Blue®“, Germany, January 2012.

[8] S. Flohrer, „Analyse der dynamischen Magnetisierungsprozesse nanokristalliner Weichmagnete“, Ph.D. dissertation, Institut für Werkstoffwissenschaften, TU Dresden, Germany, 2007.